Liquid-crystalline side-chain polymers: 2. Poly(allyl carbonates) and poly(vinyl carbonates)

Dominique Teyssié and Sylvie Boileau*
Collège de France, 11 place Marcelin Berthelot, 75231 Paris Cédex 05, France

Claude Friedrich and Claudine Noël
Laboratoire de Physicochimie Structurale et Macromoléculaire, ESPCI, 10 rue Vauquelin, 75231 Paris Cédex 05, France
(Received 3 July 1990; revised 3 September 1990; accepted 21 September 1990)

The free-radical polymerization of two families of nematic vinyl and allyl carbonates has been investigated starting from both the isotropic and nematic phases of the monomers. The thermal properties of the resulting polymers were examined by polarizing microscopy, differential scanning calorimetry and X-ray diffraction, and their microstructure was analysed by ^{13}C nuclear magnetic resonance. A change in the stereoregularity of the poly(vinyl carbonates) was observed when the polymers were prepared from the nematic phase of the monomers compared to the isotropic phase.

(Keywords: liquid crystals; vinyl carbonates; allyl carbonates; free-radical polymerization; stereoregularity)

INTRODUCTION

The polymerization of vinyl carbonates has been little investigated and developments in the field have long remained limited presumably due to difficulties in the synthesis of the monomers[1,2]. The bulk polymerization of methyl vinyl carbonate was the first reported example of free-radical initiated polymerization of vinyl carbonates[1]. A variety of initiators including azobisisobutyronitrile (AIBN) and benzoyl peroxide (BP) were studied, but led to low yields and low $\overline{M}_n$ values with monomers such as phenyl menthyl, oestradiol or t-butyl vinyl carbonates[3–5]. However, initiation by dicyclohexyl peroxydicarbonate (DCPD), introduced by Meunier *et al.*[3], gave better results and was then successfully used by other authors[5,6]. On the other hand, u.v. irradiation in the presence of a photosensitizer was also reported for the polymerization of fluorinated and chlorinated vinyl carbonates[7].

Comparatively fewer allyl carbonates were polymerized, the most important of which is diethylene glycol bisallyl carbonate, i.e. 'CR 39' widely used for optical purposes[8]. The photoinduced polymerization of this monomer was recently investigated, and it was shown that casting by irradiation can be carried out without defects in shorter cycles, leading to materials suitable for optical applications[9].

In the present report, the free-radical polymerization of a series of nematic vinyl and allyl carbonates was investigated. It was interesting to determine whether the presence of a carbonate linkage in the spacer between the mesogenic moiety and the macromolecular backbone would interfere with the occurrence of mesophases in the resulting polymers. The thermal stability of these polymers was expected to be good since poly(vinyl phenyl carbonate) is stable up to 250°C[10].

The synthesis of the monomers bearing a mesogenic core with a *p*-substituted phenyl benzoate group was described previously[11]. The properties of the polymers were examined as a function of the length and chemical nature of the terminal group on the mesogenic moiety. The effect of the length of the spacer, i.e. starting from either an allyl or a vinyl carbonate, was also examined.

On the other hand, monomer organization (in either the mesomorphous or isotropic phase or in the presence of a liquid-crystal solvent) may affect the kinetics of the polymerization and/or the microstructure of the resulting polymer. Such an effect was first reported by Amerik and Krentsel[12], who noticed a difference in the morphology of poly(vinyl oleate) according to the phase in which the monomer was polymerized. Amerik *et al.*[13] also obtained polymers of (*p*-methacryloyloxy)benzoic acid with different molar masses according to whether the polymerization was carried out in solution or in the presence of a liquid-crystal solvent. Blumstein *et al.*[14] noticed an increase in the syndiotacticity of the same polymer prepared in mesomorphic solvents with respect to the polymers obtained in bulk or in solution. However, most studies on the polymerization of liquid crystals were focused on the influence of the physical state of the monomer on the kinetics of the reaction. According to Tanaka[15], the kinetics of the polymerization of 4-(2-vinyloxyethoxy)benzoic acid is not dependent on the phases of the monomer. Cser *et al.*[16] confirmed this observation.

An opposite effect was observed by Perplies *et al.*[17], who measured a sudden increase in the overall rate of the polymerization when the melt becomes isotropic for several methacrylates and acrylates (namely the *p*-(4-methoxyphenyl iminomethylidine)phenyl ester of acrylic

* Laboratoire de Chimie Macromoléculaire associé au CNRS, URA 24

0032-3861/91/132469-13

acid). A similar trend was observed by Hoyle *et al.*[18], who noticed a higher polymerization rate of a cholesteryl methacrylate when the initial phase is mesomorphous. As stated by these authors, the effect might arise from a particularly convenient balance between order and mobility existing in the mesophase. Moreover, it now seems agreed that phase separation during the polymerization might be of great importance and that no general conclusions can be drawn as far as the polymerization rate of liquid crystals is concerned[19,20]. In this report, the polymers of vinyl and allyl carbonates were prepared from both the nematic and the isotropic phase whenever possible, and some of these compounds were also polymerized in solution for comparison. The thermal properties of these polymers as well as their microstructure were examined.

EXPERIMENTAL

Monomers

The synthesis, purification and characterization of the allyl and vinyl carbonates were described in a previous paper[11]. All the monomers show only one mesomorphous phase, which is nematic.

Polymers

In a typical experiment, 1 g of monomer was polymerized in bulk, under nitrogen and at a controlled temperature (± 1°C).

For each monomer, two different temperatures of polymerization were chosen. One experiment was carried out at about 10°C above the clearing temperature (T_{cl}), i.e. in the isotropic phase. The other polymerization was carried out at 5 to 10°C below T_{cl}, i.e. within the nematic phase.

Free-radical initiators such as DCPD, AIBN or BP could not be used because the melting temperatures of most of the monomers were well above the temperature ranges in which these initiators are commonly used. Therefore, either t-butyl perbenzoate (Trigonox C, Akzo Chemie) or t-butyl isopropyl peroxycarbonate (TBPIC, Société Châlonnaise des peroxydes organiques) were used. These two initiators are liquids at room temperature and were used as received. The molar ratio of initiator to monomer was chosen between 1 and 2%, and the initiator was introduced into the reaction mixture with a microsyringe. Some polymerizations were also carried out at 35°C in CH_2Cl_2 solution with DCPD as an initiator for comparison.

The polymerizations were stopped after 20 h except when the reaction mixture became too viscous earlier. Then 10 ml CH_2Cl_2 were added to the medium and the unreacted monomer was separated from the polymer by chromatography on silica gel columns with CH_2Cl_2 and tetrahydrofuran (THF) as eluents. The polymer was recovered by precipitation in ethanol and was then dried under high vacuum. The absence of unreacted monomer was checked by t.l.c. (CH_2Cl_2 as eluent) and by g.p.c. in THF.

Physicochemical measurements

The molar masses of the polymers were determined by g.p.c. in THF at 30°C on a Waters apparatus equipped for refractive index and u.v. detections using a polystyrene calibration curve.

The ^1H and ^{13}C n.m.r. spectra were recorded at 200 and 50.3 MHz, in $CDCl_3$ at 25°C, with an AM 200 SY Brüker apparatus.

Phase transition temperatures were measured using a differential analyser (du Pont 1090) with a scanning rate of 20°C min^{-1}. T_g was estimated from the point of intersection between the initial baseline and the sloping portion of the line obtained as the baseline shifts during the glass transition.

The textures of the mesophases were observed with a polarizing microscope (Leitz-Diavert) equipped with a programmable hot stage (Mettler FP52).

For the X-ray measurements, the samples were contained in 1 mm diameter Lindemann glass tubes. Diffraction patterns were recorded on flat films using Cu Kα radiation. A flat graphite crystal with a pinhole collimator was used as a monochromator. The sealed capillary tubes were mounted in an electrically heated oven, the temperature of which was controlled with a precision of 0.2°C using a platinum resistor as a sensing element. The sample holder was contained inside a tank evacuated to reduce air scattering. Oriented samples were obtained by drawing fibres out of the mesophase with a pair of tweezers.

RESULTS AND DISCUSSION

Synthesis of the polymers

The experimental conditions for the polymerizations, the g.p.c. characterization and the existence of a mesophase in the resulting polymers are reported in *Tables 1* and *2*. In spite of the low polymerizability of allyl compounds, only the allyl carbonate bearing a $C_6H_{13}O-$ terminal group could not be polymerized. In the vinyl carbonate series, the monomers bearing a $C\equiv N$ or a $C_6H_{13}O-$ terminal group both decomposed above T_{cl} and thus could not be polymerized in the isotropic phase.

Molar masses

The $\overline{M_n}$ values and the polydispersity indices (I_p) of the polymers determined by g.p.c. in THF are reported in *Tables 1* and *2*. The lowest $\overline{M_n}$ value (5000) roughly corresponds to a degree of polymerization ($\overline{DP_n}$) of 16 and the highest one (12 500) to a $\overline{DP_n}$ of 40 (although the use of polystyrene standards may lead to underestimated values).

Differences between polymerizations carried out in nematic or isotropic phases of the monomers

The polymer yields do not exceed 40%. However, it appears from *Tables 1* and *2* that the yields of polymerizations carried out in the nematic phase of the monomers are significantly higher than those of the polymerizations carried out in the isotropic phase (although the latter are usually performed 10 to 20°C higher). This could arise from an increase of transfer reactions at higher temperatures and a subsequent loss of low-molar-mass materials during the purification steps. We therefore compared the molar-mass distribution curves of the crude products of polymerizations carried out in the mesophase and in the isotropic phase (runs 5 and 6, *Table 1*) and similar results were observed. Moreover, two vinyl carbonates were also polymerized

Table 1 Polymerization of allyl carbonates

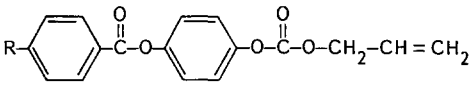

Run	R	Initiator[a]	Monomer phase[b]	T (°C)[c]	t (h)	Y (%)[d]	$\overline{M}_n$[e]	I_p[f]	Polymer mesophase
1	CH_3O–	TC	I	110	6	25	5000	1.50	+
2	C_2H_5O–	TBPIC	N	105	24	30	9900	1.55	+
3	C_2H_5O–	TBPIC	I	120	20	10	7300	1.40	+
3A	C_2H_5O–	TBPIC	I	120	17	14	7700	1.50	+
3B	C_2H_5O–	TBPIC	I	115	40	–	4600	1.70	+
3C	C_2H_5O–	TBPIC	I	115	30	33	8600	1.55	+
4	C_2H_5O–	DCPD	Sol	35	20	9	4800	1.35	+
5	C_4H_9O–	TBPIC	N	98	20	18	5300	1.90	+
6	C_4H_9O–	TBPIC	I	120	20	5	5900	1.35	+
7	–CN	TBPIC	N	115	20	30	5800	1.70	+
8	–CN	TBPIC	I	130	20	31	5500	1.45	+

[a] Initiator: TC, Trigonox C; TBPIC, t-butyl isopropyl peroxycarbonate; DCPD, dicyclohexyl peroxydicarbonate
[b] Monomer phase: I, isotropic; N, nematic; Sol, solution
[c] T (°C): temperature of polymerization
[d] Y (%): yield of purified polymer
[e] $\overline{M}_n$: determined by g.p.c. in THF using a polystyrene calibration curve
[f] I_p: polydispersity index of the polymer

Table 2 Polymerization of vinyl carbonates

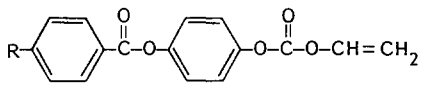

Run	R	Initiator[a]	Monomer phase[b]	T (°C)[c]	t (h)	Y (%)[d]	$\overline{M}_n$[e]	I_p[f]	Polymer mesophase
1	C_2H_5–	TC	N	90	20	20	5000	3.00	–
2	C_2H_5–	TC	I	100	20	13	7000	1.50	–
3	C_2H_5–	DCPD	Sol	35	20	13	8400	1.60	–
4	CH_3O–	TBPIC	N	120	20	12	11 800	1.50	–
5	CH_3O–	TBPIC	I	140	6	5	9200	2.60	–
6	C_2H_5O–	TC	N	140	3	20	6400	1.40	+
7	C_2H_5O–	TC	I	155	20	10	5300	1.50	+
8	C_2H_5O–	DCPD	Sol	35	20	6	6600	1.50	+
9	C_4H_9O–	TBPIC	N	117	7	35	11 800	2.15	+
10	C_4H_9O–	TBPIC	I	135	7	15	12 000	3.45	+
11	$C_6H_{13}O$–	TC	N	100	20	14	12 500	1.55	+
12	–CN	TC	N	140	0.1	40	5500	1.55	+

For abbreviations, see *Table 1*

in solution (runs 3 and 8, *Table 2*) and the polymer yields are close to those obtained in the corresponding isotropic phase polymerizations. It could thus be concluded that the overall rates of the polymerizations are higher when the reactions are carried out in the nematic phase.

The polymers were examined by ^1H and ^{13}C n.m.r. The ^{13}C chemical shifts of poly(vinyl carbonates) are reported in *Table 3*, and typical spectra of the poly(vinyl carbonate) bearing a C_2H_5O– terminal group on the mesogenic moiety are shown in *Figure 1*. The different integrations and assignments correspond to the expected formula. The ^1H and ^{13}C chemical shifts of the atoms belonging to the mesogenic groups are identical in the poly(vinyl carbonates) and in the corresponding poly(allyl carbonates).

The superposition of the ^{13}C signals from 33 to 37 ppm corresponding to the backbone carbon atoms in the poly(allyl carbonates) prevented any information on the tacticity of these polymers from being derived. However, in the poly(vinyl carbonates), the methine carbons of the backbone clearly showed a triad effect and sometimes a slight splitting corresponding to pentads. Calculations of the areas of the –CH regions leading to the proportions of iso-, hetero- and syndiotactic triads are reported in *Table 4* (the assignments of the three peaks were made

Table 3 Chemical shifts for poly(vinyl carbonates) at 50.3 MHz at 25°C in $CDCl_3$

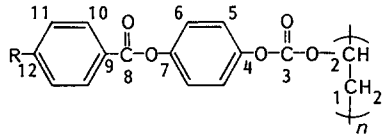

R	^{13}C chemical shift (ppm)													
	1	2[a]	3	5	6	8	10	11	13	14	15	16	17	18
CH_3–CH_2–CH_2–CH_2–CH_2–CH_2–O– (18 17 16 15 14 13)	39.7	72.0	154.3	122.0	132.0	164.2	122.6	113.8	68.1	31.5	29.1	25.5	22.5	13.9
CH_3–CH_2–CH_2–CH_2–O– (16 15 14 13)	39.6	72.2	154.3	126.7	132.1	164.3	122.5	114.1	67.8	31.1	19.1	13.6		
CH_3–CH_2–O– (14 13)	39.5	72.2	154.4	121.9	132.1	164.2	122.5	113.9	63.5	14.5				
CH_3–O– (13)	39.5	72.2	154.4	121.9	132.6	164.3	122.5	113.6	55.3					
CH_3–CH_2– (14 13)	39.6	71.8	154.3	121.8	130.3	164.5	127.3	122.5	28.8	15.04				

[a] Chemical shift of the hetero signal in the triad

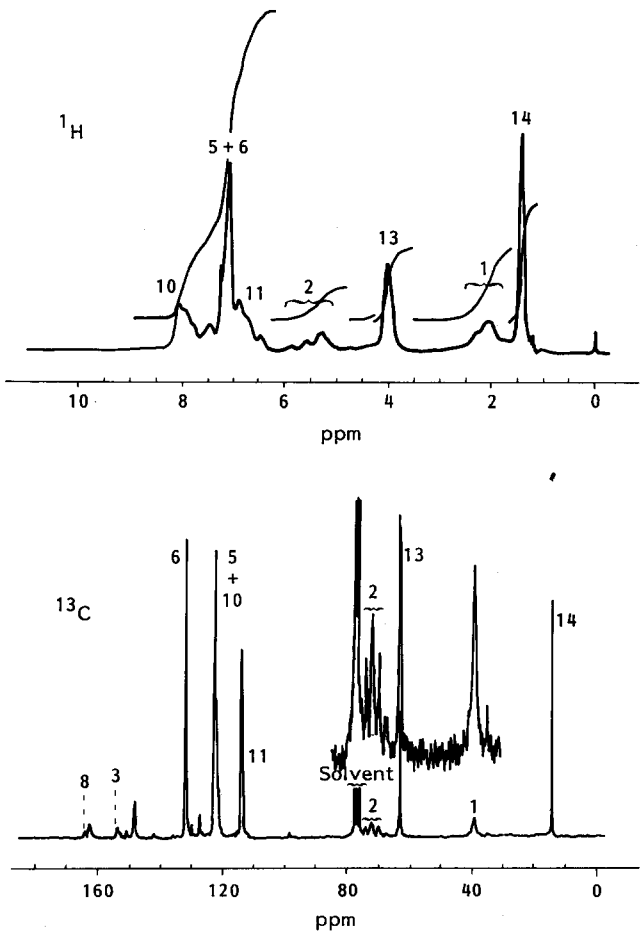

Figure 1 ^1H and ^{13}C n.m.r. spectra at 25°C in $CDCl_3$ of the following:

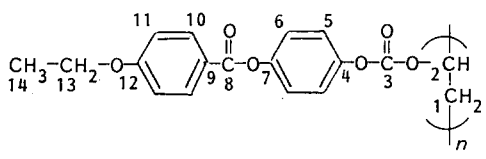

according to ref. 21). Bovey's calculations[22] lead to $P_{m/r}+P_{r/m}$ values between 0.92 and 1.02, which corresponds to Bernoullian statistics.

For the poly(vinyl carbonates) prepared from the isotropic phase of the monomer, a 1:2:1 ratio was observed for the peaks corresponding to the iso-, hetero- and syndiotactic triads. However, for the polymers obtained from the nematic phase of the monomer, an increase in the proportion of syndiotactic triads was observed. This effect is illustrated in *Figure 2*, showing the methine carbon region in the ^{13}C n.m.r. spectra of the poly(vinyl carbonates) bearing a C_4H_9O– terminal group on the mesogenic moiety. Polymerization from the nematic phase of the vinyl carbonates thus seems to promote a change in the tacticity of the polymer.

Thermal behaviour

The polymers were analysed by optical microscopy and d.s.c. For low-molecular-weight polymers, the glass transition temperature (T_g) is a function of $\overline{M}_n$. It seems that the plateau value of this curve was not reached with our polymers: in five different polymerizations of the allyl carbonates bearing a C_2H_5O– terminal group, an increase in the T_g value from 64 to 89°C was observed, corresponding to a $\overline{M}_n$ range from 4600 to 9900 (*Figure 3*). Thus, not all the transition temperatures reported in *Table 5* can be compared directly.

The poly(vinyl carbonates) and poly(allyl carbonates) exhibit very different thermal behaviours and this point will be discussed separately.

Poly(vinyl carbonates). There is no real evidence for liquid-crystal properties in the two polymers bearing the shortest terminal substituents (R = CH_3O–; C_2H_5–) on the mesogenic groups (*Table 2* runs 1–5 and *Table 5*). Rather, these polymers resemble typical amorphous polymers. Their d.s.c. traces are characterized by a marked glass transition at 110 and 120°C for R = CH_3O– and

Table 4 Proportions of different triads calculated from the ^{13}C n.m.r. spectra of the methine carbon in the poly(vinyl carbonates)

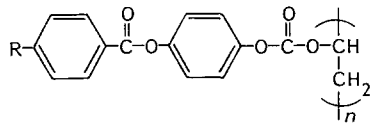

	Isotropic-phase polymerization				Nematic-phase polymerization			
R	Run	i	h	s	Run	i	h	s
CH_3–CH_2–	2	0.25	0.48	0.27	1	0.18	0.48	0.34
CH_3O–	5	0.27	0.46	0.27	–	–	–	–
CH_3–CH_2–O–	–	–	–	–	6	0.19	0.48	0.32
CH_3–$(CH_2)_3$–O–	10	0.23	0.51	0.26	9	0.20	0.47	0.33
CH_3–$(CH_2)_5$–O–	–	–	–	–	11	0.17	0.43	0.40

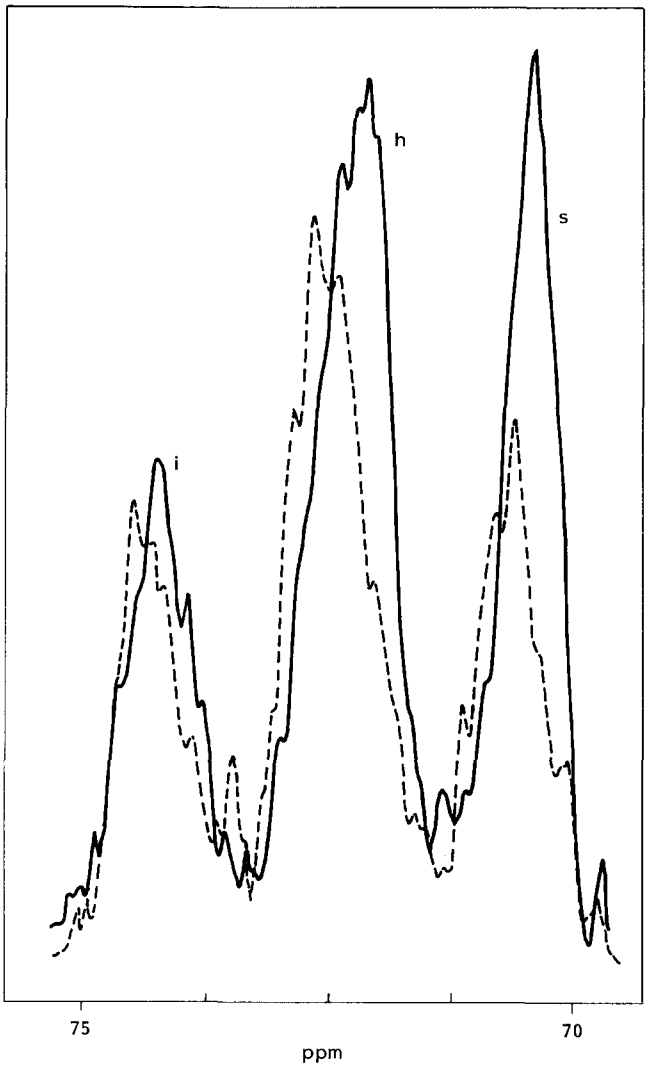

Figure 2 Enlargement of the methine carbon region in the ^{13}C n.m.r. spectra of the following, prepared in the nematic phase (——) and in the isotropic phase (– – –)

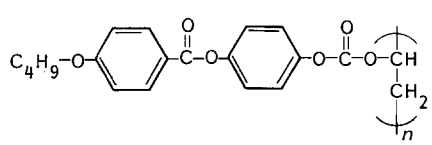

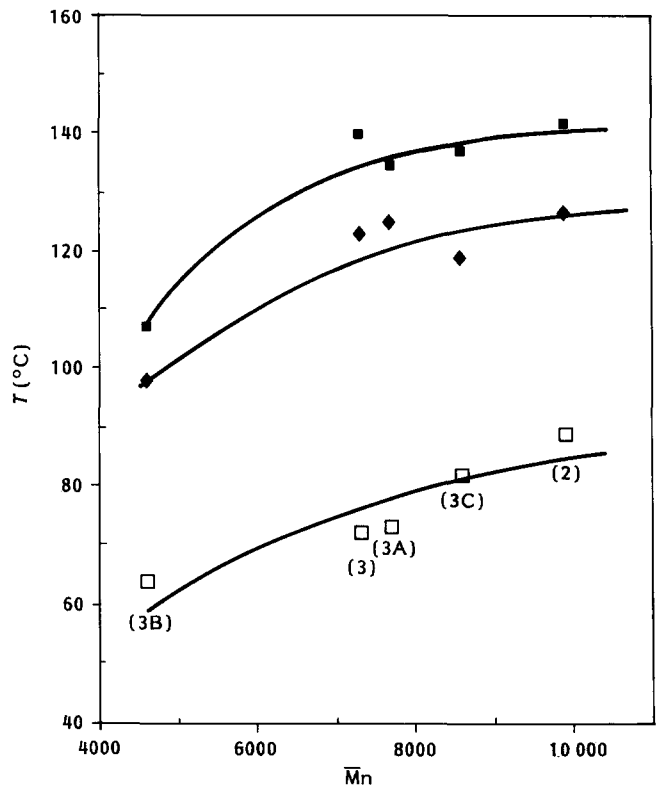

Figure 3 Dependence of the transition temperatures of the following upon $\overline{M}_n$. For each experiment, the run number is in brackets. (□) Glass transition temperature (T_g). (◆) Smectic–nematic transition temperature (T_{SN}). (■) Clearing temperature (T_{cl})

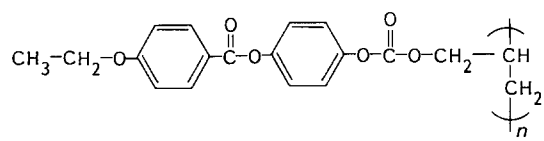

C_2H_5–, respectively. Below the glass transition no fluidity can be detected and no typical texture can be obtained. At higher temperatures, the two polymers give a clear isotropic phase. This probably results from the combination of the short terminal group and the direct attachment of the mesogenic group to the backbone via the –O–CO–O– linking unit. It seems that rigidity and

Table 5 Transition temperatures[a] (°C) determined by d.s.c. (heating rate 20°C min^{-1}) of different poly(allyl carbonates) and poly(vinyl carbonates) polymerized in the nematic or the isotropic phase of the monomer[b]

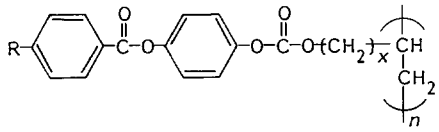

	Poly(allyl carbonates) ($x=1$) polymerized in the								Poly(vinyl carbonates) ($x=0$) polymerized in the					
	Nematic state				Isotropic state				Nematic state			Isotropic state		
R		T_g	T_{SN}	T_{cl}		T_g	T_{SN}	T_{cl}		T_g	T_{cl}		T_g	T_{cl}
C_2H_5–									(1)	120	–			
CH_3O–					(1)	70	N	135	(4)	110	–		100	–
C_2H_5O–	(2)	89 S	127 N	142	(3)	64 S	98 N	107	(6)	–	188	(5)		170
					(3A)	72 S	123 N	140		–	199			
					(3B)	73 S	125 N	135		–	187			
					(3C)	82 S	119 N	137						
C_4H_9O–	(5)	54 S	95 N	137	(6)	55 S	100 N	140	(9)	–	165	(10)	–	160
–CN	(7)	90 S	185 N	220	(8)	85 S	170 N	210						

[a] T_g: glass transition temperature; T_{SN}: smectic/nematic transition temperature; T_{cl}: clearing temperature (for poly(vinyl carbonates) this temperature was determined by optical microscopy)
[b] For each experiment, the run number is in brackets

steric hindrance create a high conformational energy barrier to mesogen packing.

The d.s.c. traces of the other poly(vinyl carbonates) are characterized by a very broad endotherm. Microscopic observations during the course of this endotherm show that the polymers melt to give a birefringent phase. However, the polymers decompose shortly after this transition, which makes it difficult to identify the mesophases. The decomposition temperatures lie in the range 210–230°C, which is consistent with the values reported in the literature for other poly(vinyl carbonates)[10].

It should be pointed out now that, except in a few cases[23–25], polymers with mesogenic groups directly attached to the backbone give only glasses with an anisotropy of structure that is lost at the glass transition[26,27]. Coupled with steric interactions between the side groups, the tendency towards a statistical distribution of chain conformations hinders the ordered arrangement of the mesogenic units and liquid-crystal formation is suppressed. It is remarkable that only small changes in the length of the terminal substituent R can dramatically affect the properties of the poly(vinyl carbonates) under study. For example, the lower homologue ($R=CH_3O$–) is amorphous while the higher homologue ($R=C_2H_5O$–) is liquid-crystalline. Early reviews on low-molar-mass liquid crystals state that molecules of mesogenic compounds should contain a moderately dipolar terminal group. The replacement of a terminal hydrogen in a molecule by another substituent enhances the potential of the system to form liquid crystals. The results in *Table 5* demonstrate that one of the roles of the terminal substituent is to reveal liquid-crystal behaviour latent in the parent system and that a proper combination of side groups and main chain can lead to liquid-crystal polymers without using a flexible spacer.

Poly(allyl carbonates). All the poly(allyl carbonates) investigated are liquid-crystalline. The d.s.c. traces are characterized by a marked glass transition below 100°C and one or two endotherms at higher temperatures corresponding to a smectic–nematic transition followed by a nematic–isotropic transition. *Figure 4a* illustrates a representative d.s.c. curve obtained for poly(allyl carbonate) where $R=CH_3$–CH_2–O–. The transition temperatures are given in *Table 5*. From this table, the following points can be established:

(i) Transition temperatures and temperature ranges of mesophase stability are larger in the polymers than in the corresponding monomers (*Figure 5*), which is consistent with most results reported so far[28].

(ii) A terminal –CN group is more favourable than an alkoxy group in promoting high T_{NI} values.

(iii) Replacement of OCH_3 by a CN group promotes smectic properties.

(iv) Longer terminal n-alkyl chains favour formation of smectic mesophases. When R=OMe, the compound is purely nematogenic. When R=OEt or OBu, the compounds show smectic in addition to nematic properties. This behaviour is very general for both low-molar-mass[29] and polymeric[30] liquid crystals.

Initial classification of the phase type was based on microscopic observations of the textures exhibited by these materials. All the poly(allyl carbonates) investigated exhibit at least a nematic phase, the textures of which are reminiscent of those of conventional liquid crystals[31]. Polarized light photomicrographs depicting the appearance of the nematic phases show readily identifiable Schlieren (*Figure 6*) and threaded (*Figures 7a–9a*) textures.

With the exception of poly(allyl carbonates) where $R=CH_3O$, the polymers also exhibit a smectic phase at lower temperatures (*Figures 7b, 8b* and *9c*). At the nematic–smectic transition a striated texture with typical

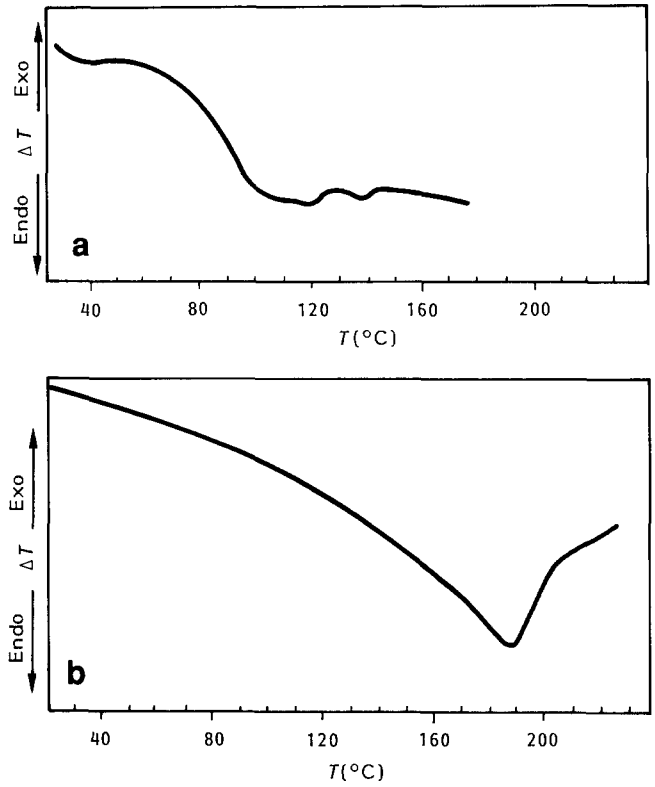

Figure 4 D.s.c. curves (heating rate 20°C min^{-1}) of (a) the following poly(allyl carbonate) and (b) the corresponding poly(vinyl carbonate)

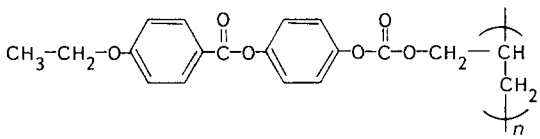

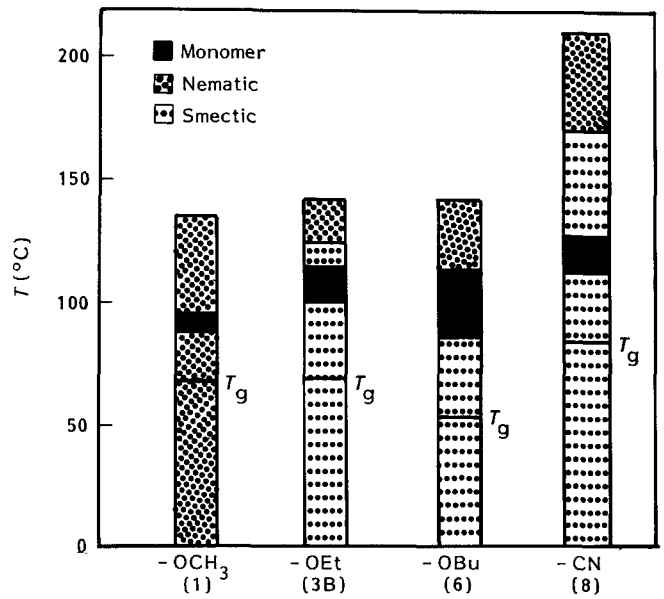

Figure 5 Temperature ranges of mesophase stability for the following allyl carbonates and the corresponding polymers in the nematic and smectic phases

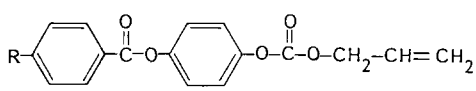

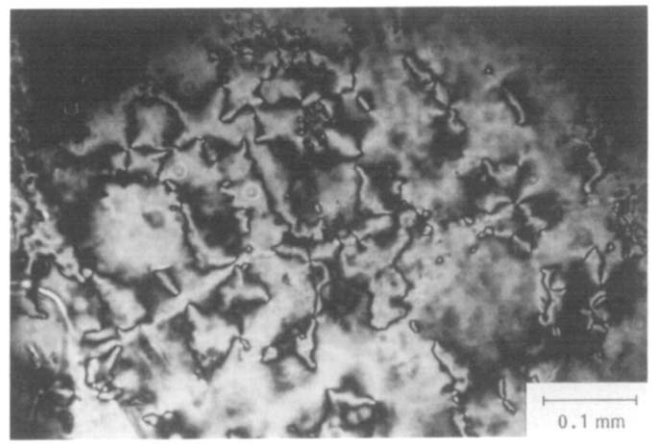

Figure 6 Schlieren texture of the following poly(allyl carbonate) at $T=100$°C. Crossed polarizers. Run 1

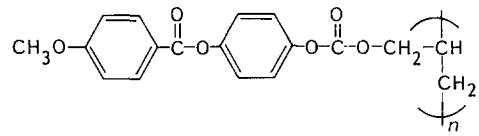

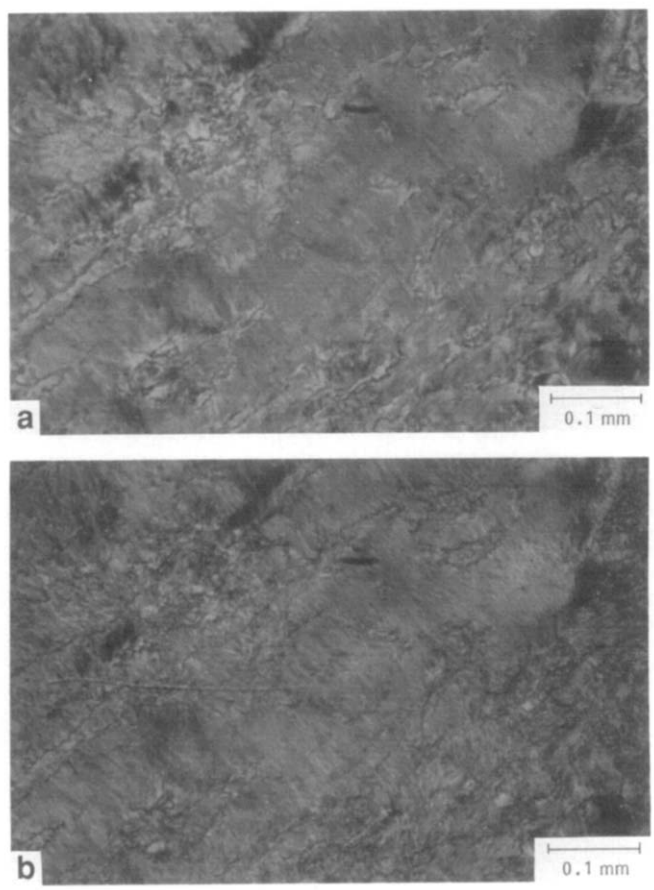

Figure 7 Textures of the nematic phase at 104°C (a) and of the smectic phase at 87°C (b) after annealing during one night. Crossed polarizers. Run 3B

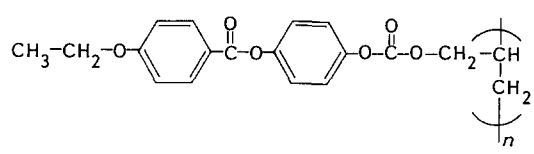

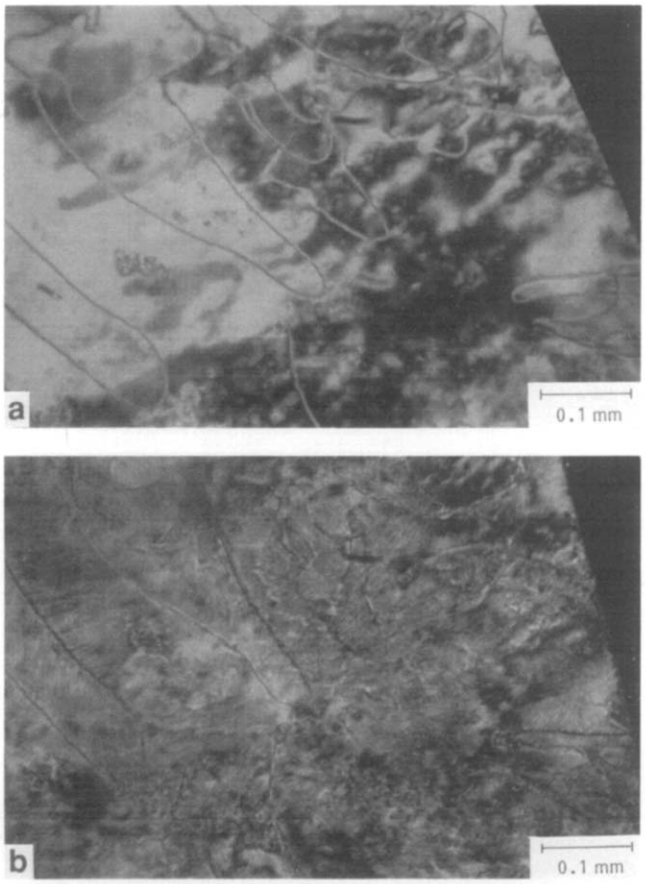

Figure 8 Threaded texture of the nematic phase at 130°C (a) and texture of the smectic phase (b) after annealing during one night at 85°C. Crossed polarizers. Run 5

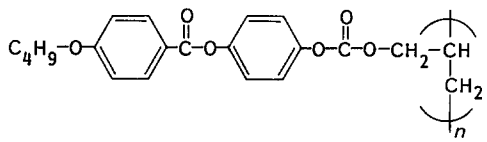

transition bars is observed (*Figure 9b*). Such a texture generally appears in the temperature range immediately below the N–S_A or N–S_C transition[31]. For poly(allyl carbonate) where R = CN this texture changes on standing for some time into the stable focal–conic fan-shaped texture, which is consistent with a S_A phase (*Figure 9c*). No typical texture could be obtained for poly(allyl carbonates) where R = –OEt or –OBu even after annealing for hours or days. This might be due to the high viscosities of the smectic state.

The assignment of nematic and smectic phases was confirmed by X-ray diffraction. Typically, the X-ray patterns obtained with powder samples of poly(allyl carbonates) where R = $C_nH_{2n+1}O$– in the nematic state consist of a broad, diffuse halo related to the lateral interferences between the mesogenic cores. It corresponds to an average intermolecular spacing of approximately 4.45–4.55 Å (*Table 6*). They present an additional diffuse ring at small angles (*Figures 10–13*). Its position corresponds to a repeat distance d that is larger than the length L of the side chain estimated for the most extended molecular configuration (*Table 6*). This effect, which is more marked for the poly(allyl carbonates) where R = OMe or OBu than for the homologue where R = OEt, will be discussed later.

In the smectic state, the poly(allyl carbonates) where R = OEt give X-ray patterns consistent with a smectic A phase (*Figure 11b*). They present a diffuse outer ring indicating a lack of periodic lateral order and two well-defined inner rings that are related to the lamellar thickness. The observed layer spacings d are almost identical with the extended model length L of the side chain so that a monolayer structure is implied (*Table 6*).

The X-ray patterns obtained using oriented fibres are qualitatively the same as those for oriented samples of

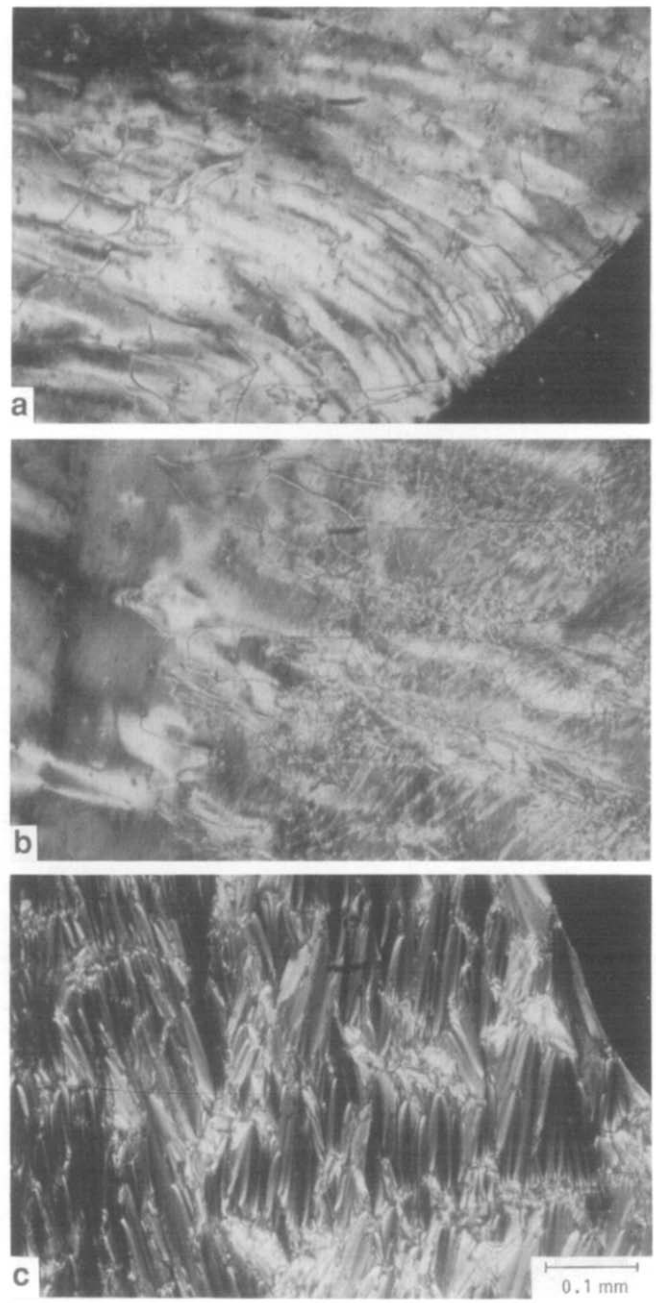

Figure 9 Threaded texture of the nematic phase at 204°C (a), striated texture at the nematic–smectic A transition (b), and focal–conic texture of the smectic A phase at 160°C (c). Crossed polarizers. Run 7

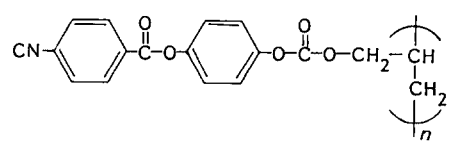

Table 6 X-ray diffraction data obtained for poly(allyl carbonates) using powder samples

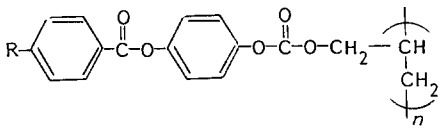

Polymer run	R	L (Å)	Nematic state d(Å)	Smectic state d(Å)
1	CH_3O	22.0	Diffuse halo 4.49 Diffuse ring 26.03	
2	C_2H_5O ($\overline{M}_n = 9900$)	23.2	Diffuse halo 4.52 Diffuse ring 26.63	Diffuse halo 4.47 Well-defined rings 24.66, 12.32
3C	C_2H_5O ($\overline{M}_n = 8600$)	23.2	Diffuse halo 4.52 Diffuse ring 25.49	Diffuse halo 4.48 Well-defined rings 24.51, 12.31
3B	C_2H_5O ($\overline{M}_n = 4600$)	25.5	Diffuse halo 4.50 Diffuse ring 25.44	Diffuse halo 4.41 Well-defined rings 24.76, 12.41
6	C_4H_9O ($\overline{M}_n = 6000$)	25.5	Diffuse halo 4.53 Diffuse ring 29.00	Diffuse halo 4.43 Well-defined ring 12.84 Diffuse ring 27.60
8	CN ($\overline{M}_n = 5600$)	21.2	Diffuse crescents 4.53 Diffuse line 16.90 Diffuse line 27.63	Diffuse halo 4.55 Bragg spots 17.19 Diffuse spots 26.81

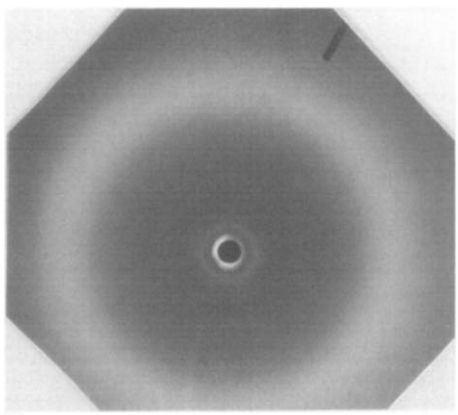

Figure 10 X-ray diffraction pattern of poly(allyl carbonate) where R = CH_3O. Nematic phase. T = 90°C

low-molar-mass smectic A phases. The anisotropy is clearly shown (*Figure 11c*) and there are correlations of two distinct periods, parallel and perpendicular to the fibre axis, which correspond to an average molecular width (≈4.4–4.5 Å) and layer thickness ($d \approx$ 24.5–24.8 Å), respectively (*Table 7*). The two symmetrical wide-angle crescents are associated with the unstructured liquid-like nature of the layers. The small-angle Bragg spots show the existence of extensive layer-like correlations. The relative position of the wide-angle crescents and the small-angle reflections with respect to the fibre axis indicates that the side chains are perpendicular to the fibre axis while the smectic layers, and as a consequence the main chain, are parallel to the direction of extension. This is consistent with most results reported so far for side-chain liquid-crystal polymers mechanically aligned by drawing fibres out of the mesophases[32–36]. The intensity of the first order of reflection is unusually low compared with the diffraction patterns of low-molar-mass liquid crystals. This is probably due to the fact that the polymer backbone and the spacer modify the electronic density and, therefore, the form factor along the normal to the layers. For a poly(methacrylate) with 4′-methoxybiphenylyl mesogenic groups and diethylene oxide spacers, Duran *et al.*[37] have shown that the electron density may have a pseudo-period of half the layer thickness by considering the polymer backbones located exactly between the biphenyl sublayers.

In addition to these common features, parallel diffuse lines, equally spaced *versus* q, are observed in a direction perpendicular to the fibre axis. This scattered intensity arises from uncorrelated periodic columns[38]. Such diffuse features do not usually appear in smectic A diffraction patterns of low-molar-mass liquid crystals. They often occur in smectic phases that exhibit three-dimensional order as, for example, smectics B, and so the most obvious explanation for their appearance in the X-ray patterns of polymers where R = OEt is in terms of a rigidity effect of the smectic layers due to the short flexible spacer used. Evidence in support of this interpretation in terms of rigidity comes from the fact that this kind of linear disorder is often observed in the smectic A or smectic C phases of side-chain liquid-crystal poly(methacrylates)[33,39,40] but does not usually appear in the diffraction patterns of their poly(acrylate) analogues[35]. For poly(allyl carbonates) where R = OEt the periodicity in this uncorrelated column is the same as the smectic layer periodicity, i.e. the extended model length L, but it is worth noting that they are out of the mean position in the layer plane.

In addition to these elements, the X-ray patterns display some weak diffuse intensity localized in four spots off the meridian. These spots are characteristic of smectic C fluctuations (usually called skewed cybotactic groups). The projection of the mean wavevector of these fluctuations along the meridian is $q_z \simeq (2\pi/45)$ Å^{-1}, which indicates that they are bilayer S_C fluctuations. It should be noted that their amplitude is quite small because these spots are very weak.

For poly(allyl carbonate) where R = C_4H_9O–, the X-ray diffraction patterns obtained with powder samples in the smectic state at 64°C are also characteristic of a

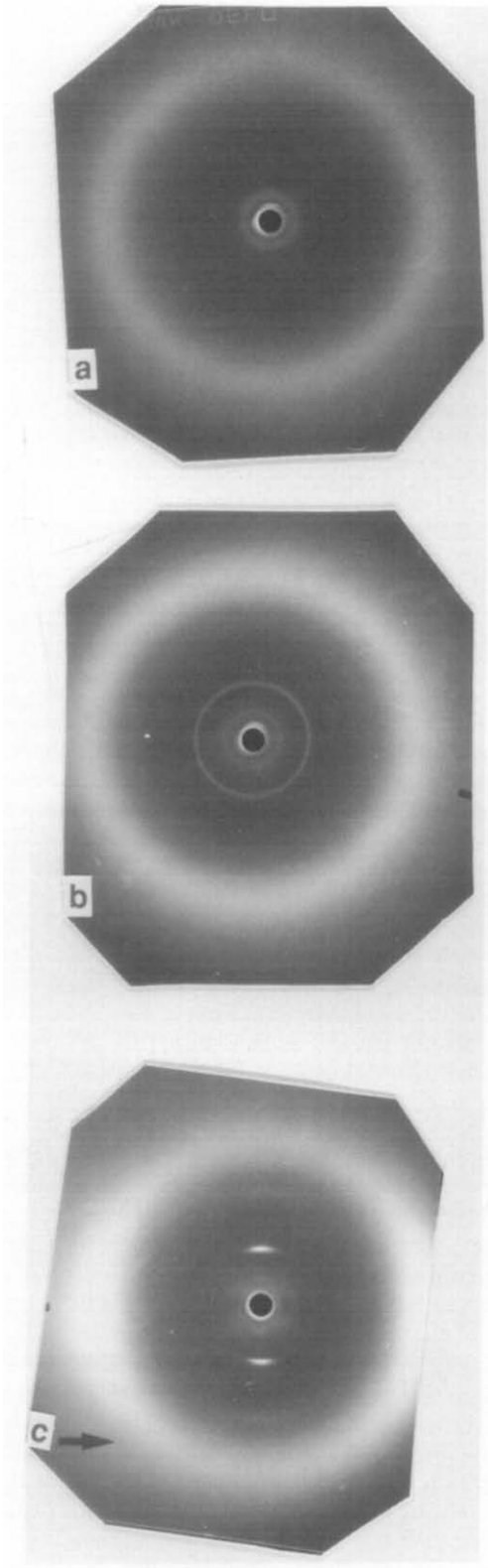

Figure 11 X-ray diffraction patterns of poly(allyl carbonate) where R = C_2H_5O. (a) Nematic phase, $T = 106$°C. (b) Smectic phase, $T = 80$°C. (c) Oriented fibre; the arrow gives the stretching direction (equator)

disordered lamellar structure (*Figure 12b*). They present in the wide-angle region a diffuse halo reflecting the absence of ordering within the layer planes and in the small-angle region a well-defined ring corresponding to a d spacing of 12.84 Å and a diffuse ring corresponding to a d spacing of 27.61 Å. The former is approximately half of the fully extended model length L, but the latter is in excess of L. The diffraction patterns obtained at higher temperatures enlightened us on these peculiarities. The sample orients spontaneously in Lindemann glass tubes (*Figure 12c*) with the director parallel to the tube axis. The outer diffuse halo splits into crescents symmetrical about the equatorial plane. The ring at 12.84 Å gives rise to two Bragg spots along the meridian. They indicate a lamellar order of periodicity $d \simeq 25.68$ Å consistent with a monolayer smectic A structure. The absence of the first order of reflection again indicates that the polymer backbone and the spacer modify the electronic density and therefore the form factor along the normal to the layers. The inner diffuse ring splits up into four spots equidistant from the origin and forming pairs aligned on straight lines making an angle of about 50–55° with respect to the director. This again is characteristic of bilayer smectic C fluctuations.

Returning to the diffraction patterns in the nematic phase (*Figure 12a* and *Table 6*), it is obvious now that the small-angle diffuse ring is connected with the existence of cybotactic groups and shows the development of enhanced order characteristic of smectic C phase.

The X-ray patterns obtained using oriented fibres are essentially the same as those described above. The anisotropy is clearly shown (*Figure 12d*) and indicates that the side chains are perpendicular to the fibre axis while the smectic layers, and as a consequence the main chains, are parallel to the stretching direction.

Poly(allyl carbonate) where R = CN orients spontaneously in the capillary tubes. The X-ray patterns obtained in the nematic state consist of two broad diffuse crescents, which are related to lateral interferences between the mesogenic cores and diffuse lines which correspond to d spacings of about 16.9 and 27.6 Å (*Figure 13a*). The former are weaker than the latter.

In the smectic A state, the X-ray patterns are characterized by two diffuse symmetrical wide-angle crescents associated with the unstructured liquid-like nature of the layers and small-angle reflections showing the existence of extensive layer-like correlations (*Figure 13b*). Only the second-order reflection corresponding to a d spacing of about 17.2 Å is seen. The layer thickness (≈ 34.4 Å) is in excess of the length of the side chains estimated for the most extended molecular conformation ($d \simeq (1.6\text{–}1.7)L$). Thus, as observed for certain low-molar-mass cyano derivatives that exhibit S_{Ad} phases[41,42], some form of bilayer structure is implied in which the side chains are partially overlapped.

In addition to these elements, the X-ray diffraction patterns display some weak diffuse intensity localized in spots off the meridian. Again, these spots are characteristic of smectic C fluctuations. The projection of the mean wavevector of these fluctuations along the meridian is $q_z \simeq (2\pi/32.7)$ Å^{-1}, which means that they are partially bilayer S_C fluctuations.

The X-ray patterns obtained from oriented fibres (*Figure 13c*) are consistent with the results described above. As observed for poly(allyl carbonates) where R = $C_nH_{2n+1}O$–, the side chains are perpendicular to the fibre axis, and the layer planes (and as a consequence the main chains) are parallel to the direction of extension. It should be noted that stretched samples of polymers having mesogenic groups with ring–CN terminal substituent and longer flexible spacer give X-ray patterns that are consistent with the side chains parallel to the fibre axis[39,43,44].

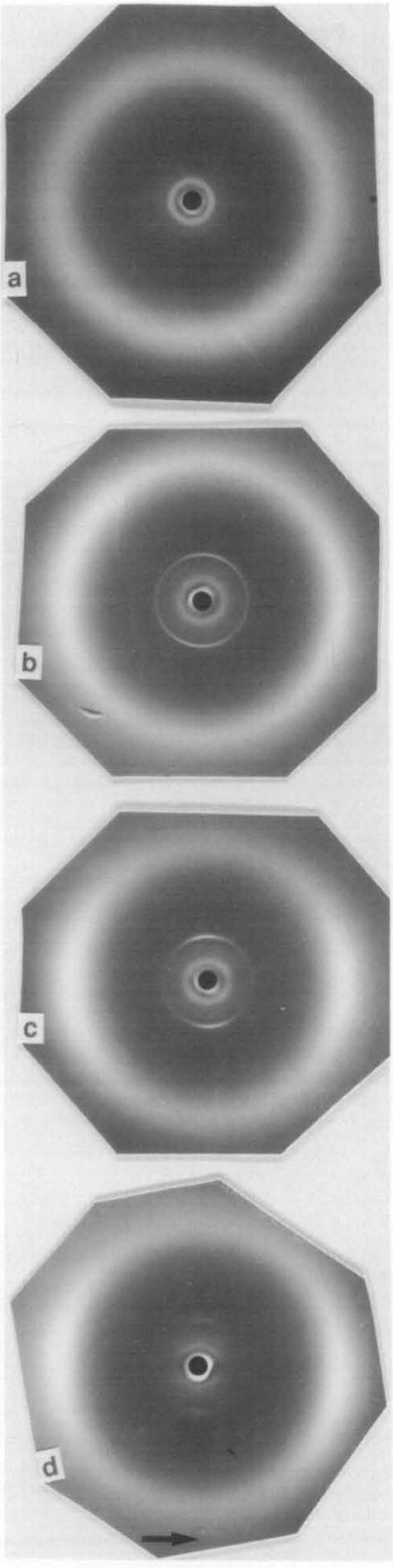

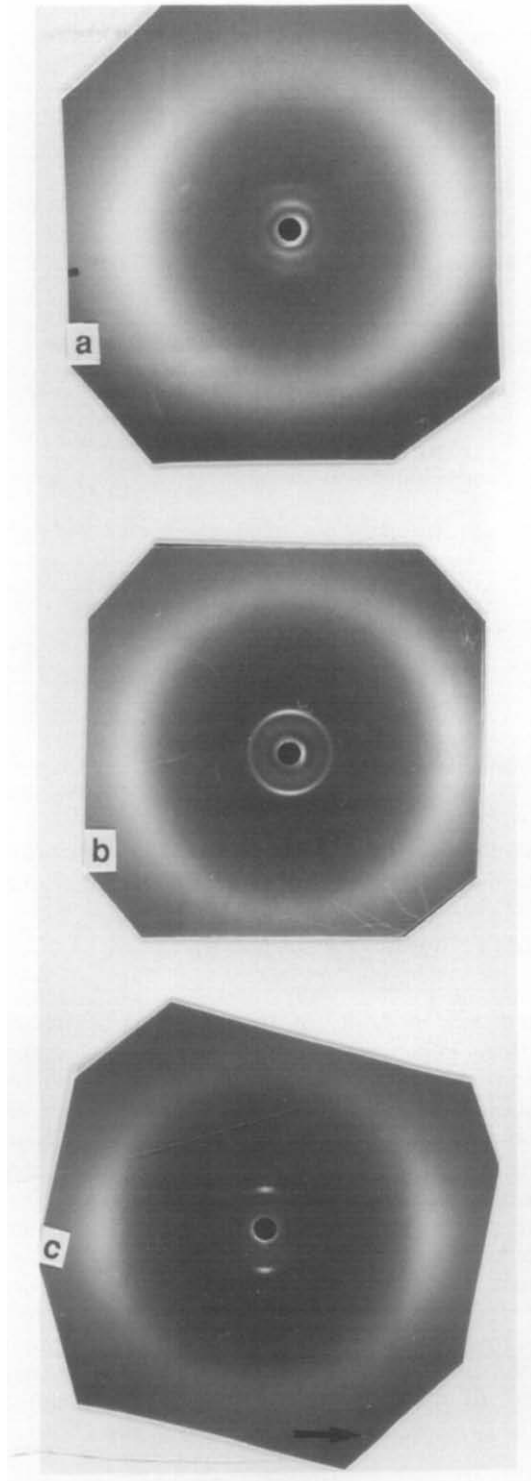

Figure 13 X-ray diffraction patterns of poly(allyl carbonate) where R = CN. (a) Nematic phase, $T = 191°C$. (b) Smectic Ad phase, $T = 115°C$. (c) Oriented fibre; the arrow gives the stretching direction (equator)

Finally it should be noted that the relative positions of the carbonate and of the methylene groups in the spacer have a determining effect on the liquid-crystalline properties of the resulting polymers. We synthesized an isomer of the allyl compound corresponding to run 2 (not

Figure 12 X-ray diffraction patterns of poly(allyl carbonate) where $R = C_4H_9O$. (a) Nematic phase, $T = 105°C$. (b) Smectic phase, $T = 64°C$. (c) Smectic phase, $T = 80°C$. (d) Oriented fibre; the arrow gives the stretching direction (equator)

Table 7 X-ray diffraction data obtained for poly(allyl carbonates) using oriented fibres

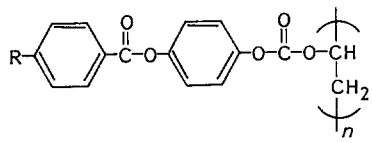

Polymer run	R	*d* (Å)
1	C_2H_5O ($\overline{M}_n$=9900)	Diffuse crescents 4.38 Bragg spots 25.05, 12.19
3C	C_2H_5O ($\overline{M}_n$=8600)	Diffuse crescents 4.42 Bragg spots 24.85, 12.32
3B	C_2H_5O ($\overline{M}_n$=4600)	Diffuse crescents 4.38 Diffuse spots 27.00 Bragg spots 25.25, 12.27, 8.13, 6.11
6	C_4H_9O ($\overline{M}_n$=6000)	Diffuse crescents 4.37 Diffuse spots 28.02 Bragg spots 12.70
8	CN ($\overline{M}_n$=5600)	Diffuse crescents 4.38 Diffuse spots 26.38 Bragg spots 17.16

described) in which the $-CH_2-$ group of the spacer was next to the phenyl ring (i.e. the carbonate and the methylene positions were reversed) and we observed that the resulting polymer has no liquid-crystalline properties at all.

CONCLUSIONS

A series of nematic vinyl and allyl carbonates were polymerized in bulk, in the presence of free-radical initiators. The polymerizations of the allyl derivatives proceed easily, probably due to the effect of the neighbouring carbonate group. The monomers bearing a cyano terminal group on the mesogenic moiety polymerize much faster and with higher yields than the other monomers.

The poly(allyl carbonates) are all liquid-crystalline, exhibiting a smectic A and/or a nematic mesophase. By contrast, in the vinyl carbonate series, the presence of a short terminal group (CH_3O- or C_2H_5-) leads to stable non-liquid-crystalline polymers. The other poly(vinyl carbonates) decompose upon heating, which makes it difficult to identify the mesophases. These results point out the determining effect of length of the spacer, i.e.

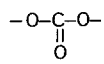

in the poly(vinyl carbonates) *versus*

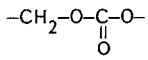

in the poly(allyl carbonates).

For a given polymer, the thermal and liquid-crystalline properties do not depend upon the physical state of the monomer (isotropic, nematic or in solution) during the course of the polymerization. The high temperatures that were necessary for carrying out bulk polymerizations (between 90 and 160°C) and the free-radical mechanism involved are probably the most important factors that control the reaction and lead to predominantly atactic polymers in these experiments. The analysis of the microstructure of the poly(vinyl carbonates) prepared from the nematic phase nevertheless suggests the appearance of a preferential tacticity. However, the differences in stereoregularity are probably not large enough to induce a distinct change in the liquid-crystalline properties of the polymers. Further work in this field is in progress.

REFERENCES

1 Kung, F. E. US Patent 1945, 2 377 085
2 Schaefgen, J. R. *J. Polym. Sci.* (*C*) 1968, **24**, 75
3 Meunier, G., Hémery, P., Boileau, S., Senet, J. P. and Cheradame, H. *Polymer* 1982, **23**, 849
4 Brosse, J. C., Cardon, F. and Soutif, J. C. *Makromol. Chem., Rapid Commun.* 1984, **5**, 95
5 Gibson, H. W. and Kurek, P. R. *Polym. Commun.* 1987, **28**, 97
6 Freine, M. T. G., Danicher, L. and Lambla, L. *Makromol. Chem.* 1988, **189**, 67
7 Boutevin, B., Pietrasanta, Y., Laroze, A. and Rousseau, A. *Polym. Bull.* 1986, **16**, 391
8 Strain, F. and Kung, F. E. US Patent 1945, 2 384 143
9 Bellobono, I. R. and Zeni, M. *Makromol. Chem., Rapid Commun.* 1986, **7**, 733
10 Kassir, F., Boivin, S., Boileau, S., Cheradame, H., Wooden, G. P. and Olofson, R. A. *Polymer* 1985, **26**, 443
11 de Marignan, G., Teyssié, D., Boileau, S., Malthête, J. and Noël, C. *Polymer* 1988, **29**, 1318
12 Amerik, Y. B. and Krentsel, B. A. *J. Polym. Sci.* (*C*) 1967, **16**, 1383
13 Amerik, Y. B., Konstantinov, I. I. and Krentsel, B. A. *J. Polym. Sci.* (*C*) 1968, **23**, 231
14 Blumstein, A., Blumstein, R. B., Clough, S. B. and Hsu, E. C. *Macromolecules* 1975, **8**, 73
15 Tanaka, Y., Hitotsuyanagi, M., Shimura, Y., Okada, A., Sakuraba, H. and Sakata, T. *Makromol. Chem.* 1976, **177**, 3035
16 Cser, F., Nyitrai, K. and Hardy, G. in 'Mesomorphic Order in Polymers' (Ed. A. Blumstein), *ACS Symp. Ser.* 1978, **74**, 95, American Chemical Society, Washington DC
17 Perplies, E., Ringsdorf, H. and Wendorff, J. H. *Makromol. Chem.* 1974, **175**, 553
18 Hoyle, C. E., Chawla, C. P. and Griffin, A. C. *Polymer* 1989, **60**, 1909
19 Paleos, C. M. *Chem. Soc. Rev.* 1985, **14**, 45
20 Blumstein, A. in 'Polymerization of Organized Systems' (Ed. H. G. Elias), Gordon and Breach, New York, 1977, p. 133
21 Meunier, G. Thèse de Docteur-Ingénieur, Paris, 1981
22 Bovey, F. A. 'High Resolution NMR of Macromolecules', Academic Press, New York, 1972
23 Perplies, E., Ringsdorf, H. and Wendorff, J. H. *J. Polym. Sci., Polym. Lett. Edn.* 1976, **13**, 243
24 Cser, F. and Nyitrai,K. *Magy. Kem. Foly.* 1976, **82**, 207
25 Shibaev, V. P., Freidzon, J. S. and Platé, N. A. *Dokl. Akad. Nauk SSSR* 1976, **227**, 1412
26 Shibaev, V. P. and Platé, N. A. *Vysokomol. Soed.* (*A*) 1977, **19**, 23
27 Blumstein, A. and Hsu, E. C. in 'Liquid Crystalline Order in Polymers' (Ed. A. Blumstein), Academic Press, New York, 1978
28 Finkelmann, H. in 'Polymer Liquid Crystals' (Eds. A. Ciferri, W. R. Krigbaum and R. B. Meyer), Academic Press, New York, 1982, p. 35
29 Gray, G. W. in 'Liquid Crystals and Plastic Crystals' (Eds. G. W. Gray and P. A. Winsor), Horwood, Chichester, 1974, vol. 1, p. 103
30 Noël, C. *Makromol. Chem., Macromol. Symp.* 1988, **22**, 95
31 Demus, D. and Richter, L. 'Textures of Liquid Crystals', Verlag Chemie, Weinheim, 1978
32 Zentel, R. and Strobl, G. R. *Makromol. Chem.* 1984, **185**, 2669
33 Decobert, G., Dubois, J. C., Esselin, S. and Noël, C. *Liquid Cryst.* 1986, **1**, 307
34 Zugenmaier, P. *Makromol. Chem., Macromol. Symp.* 1986, **2**, 33
35 Esselin, S., Bosio, L., Noël, C., Decobert, G. and Dubois, J. C. *Liquid Cryst.* 1987, **2**, 505
36 Sutherland, H.H., Basu, S. and Rawas, A. *Mol. Cryst. Liq. Cryst.* 1987, **145**, 73
37 Duran, R., Guillon, D., Gramain, P. and Skoulios, A.

J. Physique 1988, **49**, 1455

38 Doucet, J., Levelut, A. M. and Lambert, M. *Mol. Cryst. Liq. Cryst.* 1973, **24**, 317; Doucet, J. in 'The Molecular Physics of Liquid Crystals' (Eds. G. R. Luckhurst and G. W. Gray), Academic Press, New York, 1979, Ch. 14, p. 317

39 Davidson, P., Keller, P. and Levelut, A. M. *J. Physique* 1985, **46**, 939

40 Davidson, P., Decobert, G., Soyer, F. and Dubois, J. C. *Polym. Bull.* 1985, **14**, 549

41 Hardouin, F., Levelut, A. M., Achard, M. F. and Sigaud, G. *J. Chim. Phys.* 1983, **80**, 53

42 Leadbetter, A. J., Frost, J. C., Gaughan, J. P., Gray, G. W. and Mosley, A. *J. Physique* 1979, **40**, 375

43 Le Barny, P., Ravaux, G., Dubois, J. C., Parneix, J. P., Njeumo, R., Legrand, C. and Levelut, A. M. in 'Molecular and Polymeric Optoelectronic Materials: Fundamentals and Applications' (Proc. SPIE 682), San Diego, 1986

44 Noël, C., Friedrich, C., Leonard, V., Le Barny, P., Ravaux, G. and Dubois, J. C. *Makromol. Chem., Macromol. Symp.* 1989, **24**, 283